



# One-step synthesis of highly monodisperse hybrid silica spheres in aqueous solution

Tian-Song Deng, Qi-Feng Zhang, Jun-Yan Zhang, Xin Shen, Kong-Tao Zhu, Jin-Lei Wu \*

Key Laboratory for the Physics and Chemistry of Nanodevices, Department of Electronics, Peking University, Beijing 100871, People's Republic of China

## ARTICLE INFO

### Article history:

Received 19 July 2008

Accepted 23 September 2008

Available online 30 September 2008

### Keywords:

Monodisperse

Hybrid silica spheres

Homogeneous nucleation

Growth

## ABSTRACT

An effective and reproducible method of preparing highly monodisperse organic–inorganic hybrid silica spheres was studied. One process, one precursor (organosilane) and one solvent (water) were used in our experiments. The size of hybrid silica spheres could be adjusted from 360 to 770 nm with relative standard deviation below 2% by controlling the concentration of the organosilane precursor and the ammonia catalyst. The increasing of the precursor concentration increases the particle size while the catalyst concentration has a reverse effect on the particle size. The concept of homogeneous nucleation and growth processes are introduced to explain the formation mechanism and the effect of reaction conditions. The scanning electron microscopy (SEM) images illustrate the copiousness in quantity and the uniformity in size/shape of the particles that could be routinely accomplished in this synthesis. Fourier transform infrared (FT-IR) and  $^{29}\text{Si}$  nuclear magnetic resonance (NMR) spectra confirm the structure of vinyl hybrid silica spheres, where the vinyl group ( $-\text{CH}=\text{CH}_2$ ) exists and connects to the silicon atom. This method has also been extended to design and prepare other organic–inorganic hybrid materials especially in monodisperse surface-modified silica spheres.

© 2008 Elsevier Inc. All rights reserved.

## 1. Introduction

In recent years, design and preparation of organic–inorganic hybrid materials have attracted considerable attention in the chemical synthesis [1,2]. Organic–inorganic hybrid materials are used in the biocatalyst [3–5], the surface modification [6–8], and the graft [9–13]. In the organic–inorganic hybrid materials, synthesis of the monodisperse surface-modified silica spheres is widely studied for their modified functionalities [14,15] and extensive applications in photonic crystals [16–19]. During the synthesis, the starting mixtures often include different triethoxysilanes (RTES) or trimethoxysilanes (RTMS), where the organic substitute R was varied from methyl, phenyl, octyl to vinyl [7,14,20]. In the procedures, monodisperse pure silica spheres which synthesized by tetraethyl orthosilicate (TEOS) (Stöber method) [21], are used as a substrate material in reaction mixture, e.g. Wang et al. prepared monodisperse sub-micrometer silica spheres to fabricate near-infrared photonic crystals by modifying the surface of silica with organic groups [16–19].

However, the reaction systems are too complex while using ethanol/methanol–water based systems or adding some surfac-

tants, and the precursors commonly contain two materials (silane and TEOS) [7,8]. The procedures need two or even more inconvenient processes [3–5,14–18]. It leads to two main problems that the monodispersity and particle size could not be controlled easily.

In related studies, Lee et al. [20] have synthesized silica particles using a sol–gel reaction without adding ethanol, and the precursor was only one material and no surfactants were used. Here, we enhanced this method for preparing highly monodisperse organic–inorganic hybrid silica spheres synthesized by an organosilane with controllable size in aqueous solution. The method has several main advantages. First, it is very simple and convenient that we use only one process, one precursor and one solvent. In most previous reports, both organosilane and TEOS were used as precursors with ethanol/methanol and water as solvents. Moreover, a few surfactants need to be added. Compared to the traditional method, we used an organosilane as precursor and water as solvent, and no surface modification or addition of surfactant was necessary. Second, it well controls the size, uniformity and stability of hybrid silica spheres. The size of hybrid silica spheres ranging from 360 to 770 nm with relative standard deviation ( $\sigma_r$ ) below 2% were obtained through strict control of the concentration of precursor and catalyst. The spheres which synthesized at room temperature were stable because the organic groups were not destroyed. Furthermore, the precursor has self-hydrolysis ability to realize homogeneous nucleation of silica, fast reaction rate and reproducibility.

\* Corresponding author. Fax: +86 10 62761333.

E-mail addresses: qfzhang@pku.edu.cn (Q.-F. Zhang), jacintazjy@pku.edu.cn (J.-Y. Zhang), shenxin05@pku.edu.cn (X. Shen), ktzhu@pku.edu.cn (K.-T. Zhu), jlwu@pku.edu.cn (J.-L. Wu).

## 2. Materials and methods

### 2.1. Materials

Vinyltriethoxysilane (VTES, 95%), (3-mercaptopropyl)trimethoxysilane (MPTMS, 95%) and phenyltriethoxysilane (PTES, 98%) were purchased from Alfa Aesar A Johnson Matthey Company. Tetraethyl orthosilicate (TEOS, 95%), Tween 20 and ammonia solution ( $\text{NH}_3 \cdot \text{H}_2\text{O}$ , 25%) were purchased from Sinopharm Chemical Reagent Beijing Co., Ltd. All chemicals were used as received without further purification. Ultrapure water (18.2 M $\Omega$  cm) is used directly from a Milli-Q water system.

### 2.2. Synthesis

The monodisperse spherical colloids of hybrid silica were synthesized by using a sol-gel reaction in aqueous solution. In a typical procedure for the preparation of hybrid silica spheres, 3 mL VTES was added in 50 mL  $\text{H}_2\text{O}$  under vigorous magnetic stirring (300 rpm) for  $\sim 2$  h. Then the organic droplets were completely dissolved and a transparent solution was obtained. Under the constant magnetic stirring rate, 0.2 mL ammonia was consecutively added to the reaction mixture and the reaction was allowed to proceed at room temperature for  $\sim 1$  h. The mixture contained 0.27 mol/L VTES and 0.20 mol/L  $\text{NH}_3$ . After the completion of the reaction, in order to remove impurities, such as ammonia, water, and unreacted VTES, the resulting particles were separated from the reaction medium by repeated centrifugation (3000 rpm) and ultrasonic dispersion (using ethanol) cycles, and then redispersed in ethanol for further usage. Furthermore, in order to control the size and monodisperse of hybrid silica spheres, the concentration of VTES/ammonia was changed in our studies. The experimental details are listed in Table 1. The MPTMS/PTES hybrid silica spheres were fabricated by 3 mL MPTMS/PTES (for PTES, 1.5 mL Tween 20 was added). The processes were the same as the VTES synthesis. The pure silica spheres were synthesized by a modified Stöber method [21] to be used for a contrast in infrared analysis of the hybrid silica spheres. A 5 mL ethanol solution of TEOS was added to a 35 mL ethanol solution of water and ammonia. The 40 mL mixture containing 0.3 mol/L TEOS, 2.3 mol/L  $\text{H}_2\text{O}$ , and 1 mol/L  $\text{NH}_3 \cdot \text{H}_2\text{O}$  was stirred at room temperature for 6 h.

### 2.3. Characterization

The morphology was observed using a field emission gun scanning electron microscope (SEM) (Tecnai XL30 SFEG). The sizes

**Table 1**

Mean diameters ( $\bar{x}$ ) and relative standard deviation ( $\sigma_r$ )<sup>a</sup> of silica spheres obtained under different conditions.

Sample	Organo-silane	Precursor (mL)	Ammonia (mL)	pH value <sup>b</sup>	$\bar{x}$ (nm)	$\sigma_r$ (%)
1	VTES	0.8	0.1	10.84	–	–
2	VTES	1	0.1	10.84	436	1.34
3	VTES	3	0.1	10.84	587	1.03
4	VTES	5	0.1	10.84	774	0.73
5	VTES	3	0.025	10.60	748	1.21
6	VTES	3	0.2	11	513	1.47
7	VTES	3	0.5	11.23	439	1.80
8	VTES	3	5	11.72	361	1.90
9	MPTMS	3	0.1	10.84	1282	1.33
10	PTES	3	0.1	10.84	830	3.80

<sup>a</sup> The mean diameters ( $\bar{x}$ ) and relative standard deviation ( $\sigma_r$ ) of silica spheres are defined by statistics.  $\bar{x} = \frac{\sum_{i=1}^n x_i}{n}$ ,  $\sigma = \sqrt{\frac{\sum_{i=1}^n (x_i - \bar{x})^2}{n-1}}$ ,  $n > 5$ ,  $\sigma_r = \frac{\sigma}{\bar{x}} \times 100\%$ , where  $x_i$  is the diameter gained by measuring  $n$  spheres (about two hundred) for each sample using SEM,  $\bar{x}$  is the mean diameter,  $\sigma$  is the standard deviation and  $\sigma_r$  is the relative standard deviation.

<sup>b</sup> The pH value was detected by a Microprocessor pH Meter (pH 211, HANNA Instruments) under the room temperature ( $22 \pm 1^\circ\text{C}$ ).

of the hybrid silica spheres were measured using SEM (about two hundred spheres for each sample). A Fourier transform infrared (FT-IR) spectroscopy spectrometer Nicolet Magna-IR 750 (with Nicolet NicPlan IR Microscope) was used for infrared analysis of the hybrid silica spheres. The scanned wavenumber range is 4000–650  $\text{cm}^{-1}$ . The solid-state  $^{29}\text{Si}$  CP-MAS (CP: cross polarization, MAS: magic angle spinning) NMR spectra of hybrid silica spheres were carried out on a Bruker AV 300 spectrometer.

## 3. Results and discussion

Fig. 1a shows the SEM image of a typical sample prepared using sol-gel process. This image clearly illustrates the abundance in quantity and the uniformity in size/shape that could be routinely accomplished in this synthesis. A closer look (the inset) revealed that the surfaces of these spherical colloids were smooth. For comparison, the SEM image of pure silica spheres was given, as seen in Fig. 1b.

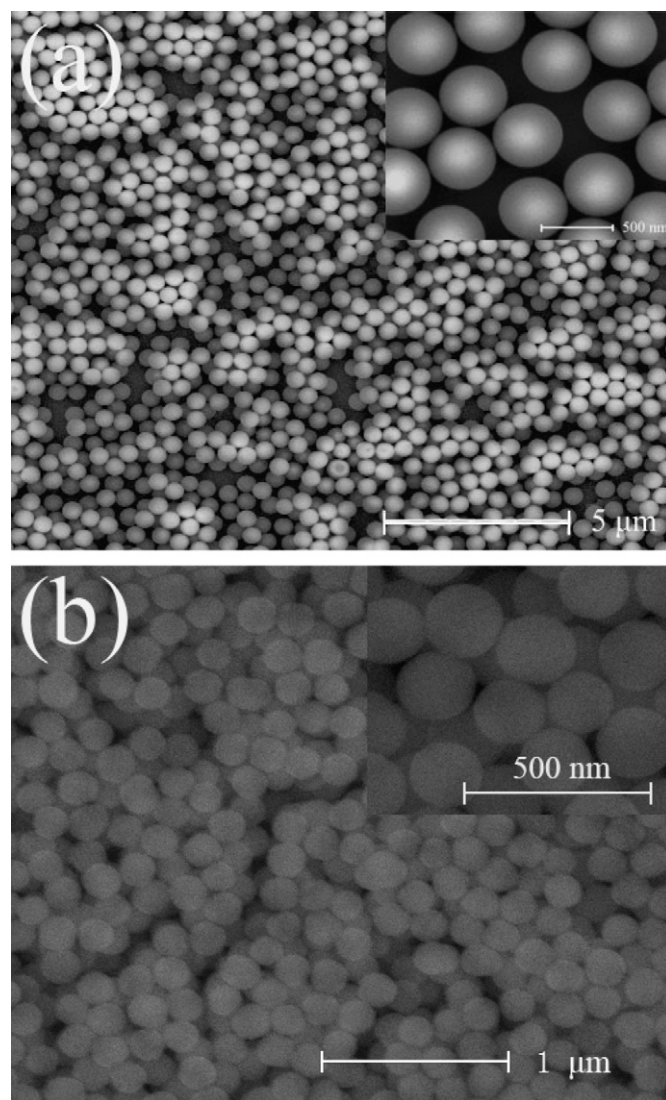


**Fig. 1.** (a) SEM image of VTES hybrid silica spheres (513 nm in mean diameter) fabricated by 3 mL VTES and 50 mL  $\text{H}_2\text{O}$  by adding 0.2 mL ammonia solution. The inset revealed that the surfaces of these spherical colloids were smooth. The reaction was carried out under constant stirring rate at room temperature ( $22 \pm 1^\circ\text{C}$ ). (b) SEM image of pure silica spheres synthesized by a modified Stöber method. The inset showed the high resolution of the same sample.

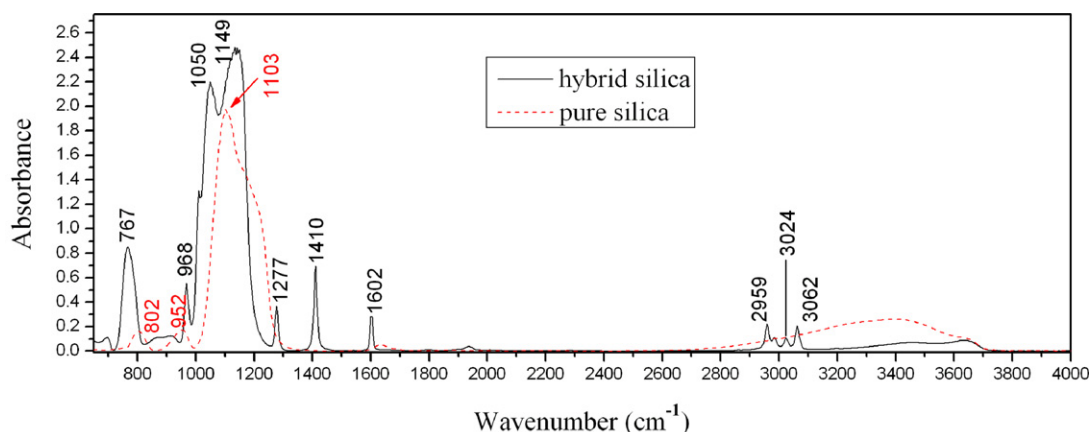


Fig. 2. FT-IR spectra of hybrid silica spheres and pure silica spheres.

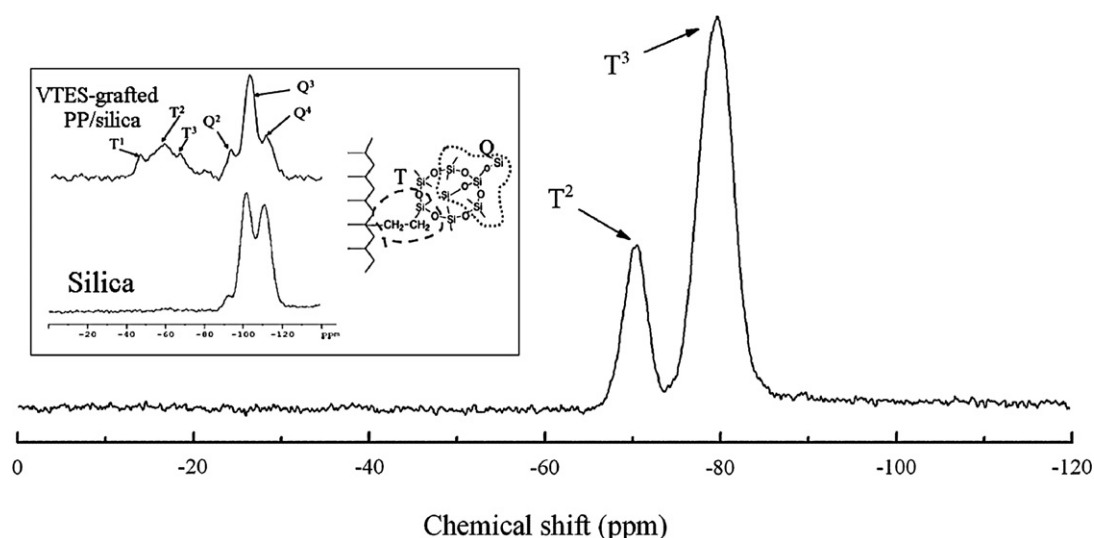


Fig. 3. Solid-state  $^{29}\text{Si}$  CP-MAS NMR spectrum of hybrid silica spheres. The inset: MAS  $^{29}\text{Si}$  NMR spectra of a (VTES-grafted PP)/silica nanocomposite and pure silica (the cartoon shows the T and Q-type structures) from Ref. [10].

### 3.1. Structural characterization of hybrid silica spheres

The chemical structure of hybrid silica spheres was studied by FT-IR and solid-state  $^{29}\text{Si}$  CP-MAS NMR spectroscopy. The FT-IR spectra in Fig. 2 illustrate the vinyl-silica spheres and pure silica spheres. According to the literatures [10,22,23] and IR spectra handbooks, the spectra in  $\sim 3700\text{--}\sim 3100\text{ cm}^{-1}$  band corresponding to the broadening OH stretching vibration illustrate that there are more OH groups in the pure silica spheres as some OH groups are replaced by  $\text{CH}=\text{CH}_2$  groups in the hybrid silica spheres. Peaks at  $3062\text{ cm}^{-1}$  and  $2959\text{ cm}^{-1}$  correspond to asymmetrical and symmetrical stretching vibrations of  $=\text{CH}_2$ , while peak at  $3024\text{ cm}^{-1}$  corresponds to  $=\text{CH}$  stretching vibration, respectively. The peak at  $1602\text{ cm}^{-1}$  is ascribed to  $\text{C}=\text{C}$  stretching vibration. The strong Si–O–Si stretching vibration band at  $1103\text{ cm}^{-1}$  in pure silica is split into two peaks ( $1050$  and  $1149\text{ cm}^{-1}$ ) in hybrid silica because the Si–C bond destroys the symmetry of Si–O–Si structure. Si–C stretching vibration band appears at  $767\text{ cm}^{-1}$ . These absorbing peaks confirm that the vinyl group ( $-\text{CH}=\text{CH}_2$ ) exists and connects to the silicon atom in the hybrid silica.

The solid-state  $^{29}\text{Si}$  CP-MAS NMR spectrum of vinyl-silica spheres is shown in Fig. 3. According to the literatures [24–27], the T species originate from the monomer, where the silicon atom is coordinated by three oxygen atoms ( $\text{T}^x: \text{RSiO}_x(\text{OH})_{3-x}$ , R: organic group). The Q species originate from TEOS, in which the silicon

atom is coordinated by four oxygen atoms ( $\text{Q}^x: \text{SiO}_x(\text{OH})_{4-x}$ ). In our experiment, the T species originate from the VTES, having four classes of T species:  $\text{T}^0$  ( $\text{CH}_2=\text{CHSi}(\text{OH})_3$ ),  $\text{T}^1$  ( $\text{CH}_2=\text{CHSiO}(\text{OH})_2$ ),  $\text{T}^2$  ( $\text{CH}_2=\text{CHSiO}_2(\text{OH})$ ), and  $\text{T}^3$  ( $\text{CH}_2=\text{CHSiO}_3$ ).

The  $^{29}\text{Si}$  NMR spectrum shows two peaks of T species, due to  $\text{T}^2$  ( $-70.5\text{ ppm}$ ) and  $\text{T}^3$  ( $-79.6\text{ ppm}$ ). The inset in Fig. 3 indicates the Jain's work [10]. They used two steps to modify the surface of silica with vinyl groups. Only Q species' peaks appeared in pure silica, and VTES-grafted PP/silica had both the Q and T species (see the inset in Fig. 3). But the intensity of Q species was stronger than the T species, indicating that the quantity of vinyl groups was limited. In our one-step direct synthesis of vinyl-silica spheres, only  $\text{T}^2$  and  $\text{T}^3$  peaks appeared in the  $^{29}\text{Si}$  NMR spectrum, indicating that the surface had abundant vinyl groups. Moreover, the area of  $\text{T}^3$  unit was about 3.5 times of  $\text{T}^2$  unit's. It provided another important proof that a majority of OH groups were replaced by  $\text{CH}=\text{CH}_2$  groups in the hybrid silica spheres. These results are consistent with FT-IR analysis.

### 3.2. Control over the size and uniformity of hybrid silica spheres

It is very important to control the monodispersity of the surface-modified silica spheres [16–18]. For instance, the monodispersity of spherical particle is critical for a good assembly in the preparation of photonic crystals [28]. Generally, the size of hybrid silica spheres depends on a number of parameters that include,



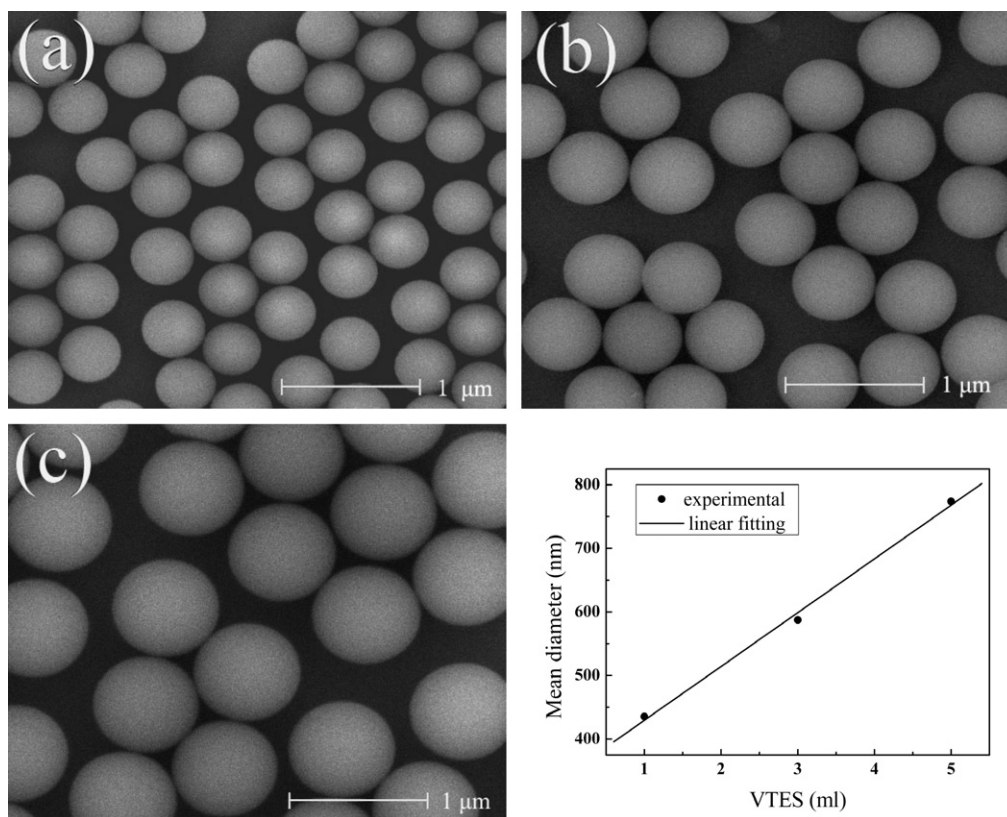


**Fig. 4.** SEM images of monodisperse hybrid silica spheres prepared adding 0.1 mL ammonia in 50 mL VTES/H<sub>2</sub>O mixture by using various amounts of VTES: (a) 1 mL, (b) 3 mL and (c) 5 mL, respectively. The resultant particle sizes are (a) 436 nm, (b) 587 nm, and (c) 774 nm. The plot shows a linear dependence between the particle size and the amount of VTES. The reaction was carried out under constant stirring rate at room temperature ( $22 \pm 1^\circ\text{C}$ ).

for example, the concentration of VTES precursor/ammonia catalyst, the ratios of water and VTES, the amount of water solvent, the stirring rate, the temperature, and the reaction time. Herein, we focus the parameters on the reaction time and the concentration of VTES/ammonia, respectively. All the reactions were allowed to proceed at room temperature ( $22 \pm 1^\circ\text{C}$ ) under the constant stirring rate.

### 3.2.1. Influence of the reaction time

We took out the reaction mixture after the ammonia was added in the VTES/water transparent solution for 5 min, and the resultant particle size and monodispersity were almost the same as the final result when the reaction was allowed to proceed for 1 h or even longer time. This observation implies that the reaction accomplished in a few minutes after the presence of ammonia. The monodisperse hybrid silica spheres could be obtained in a relatively short reaction time compared with the conventional Stöber method [29].

### 3.2.2. Influence of the concentration of VTES precursor

The concentration of VTES was found to have significant influence on the size of hybrid silica spheres, that was, the size of spheres increased with the increasing concentration of the precursor. Fig. 4 shows the SEM images of monodisperse hybrid silica spheres with various amounts of the VTES. The plot in Fig. 4 shows a linear dependence between the particle size and the amount of VTES. By altering the amount of VTES from 1 to 5 mL, the size of hybrid silica spheres could be varied in the range from ~440 to ~770 nm. It should be pointed out that the amount of VTES cannot be too small. When the amount of VTES was reduced below 1 mL, the hybrid silica colloids derived from the VTES seemed to be insufficient to form the spherical particle and appearing the rough surface, as seen in Fig. 5. To get the smooth and spherical

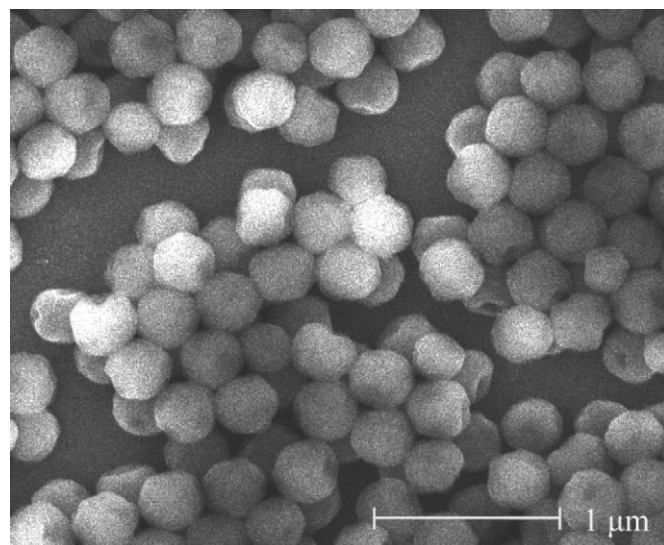


**Fig. 5.** SEM image of hybrid silica prepared using 0.8 mL VTES in 50 mL H<sub>2</sub>O by adding 0.1 mL ammonia. The reaction was carried out under constant stirring rate at room temperature ( $22 \pm 1^\circ\text{C}$ ).

silica particles, the volume ratio of the VTES and water should be above 1:50.

### 3.2.3. Influence of the concentration of ammonia catalyst (pH value)

In addition to the concentration of VTES, we found that it was convenient and reproducible to control particle size and monodispersity systematically by adjusting the concentration of ammonia catalyst (pH value). Fig. 6 shows the influence of the pH value on

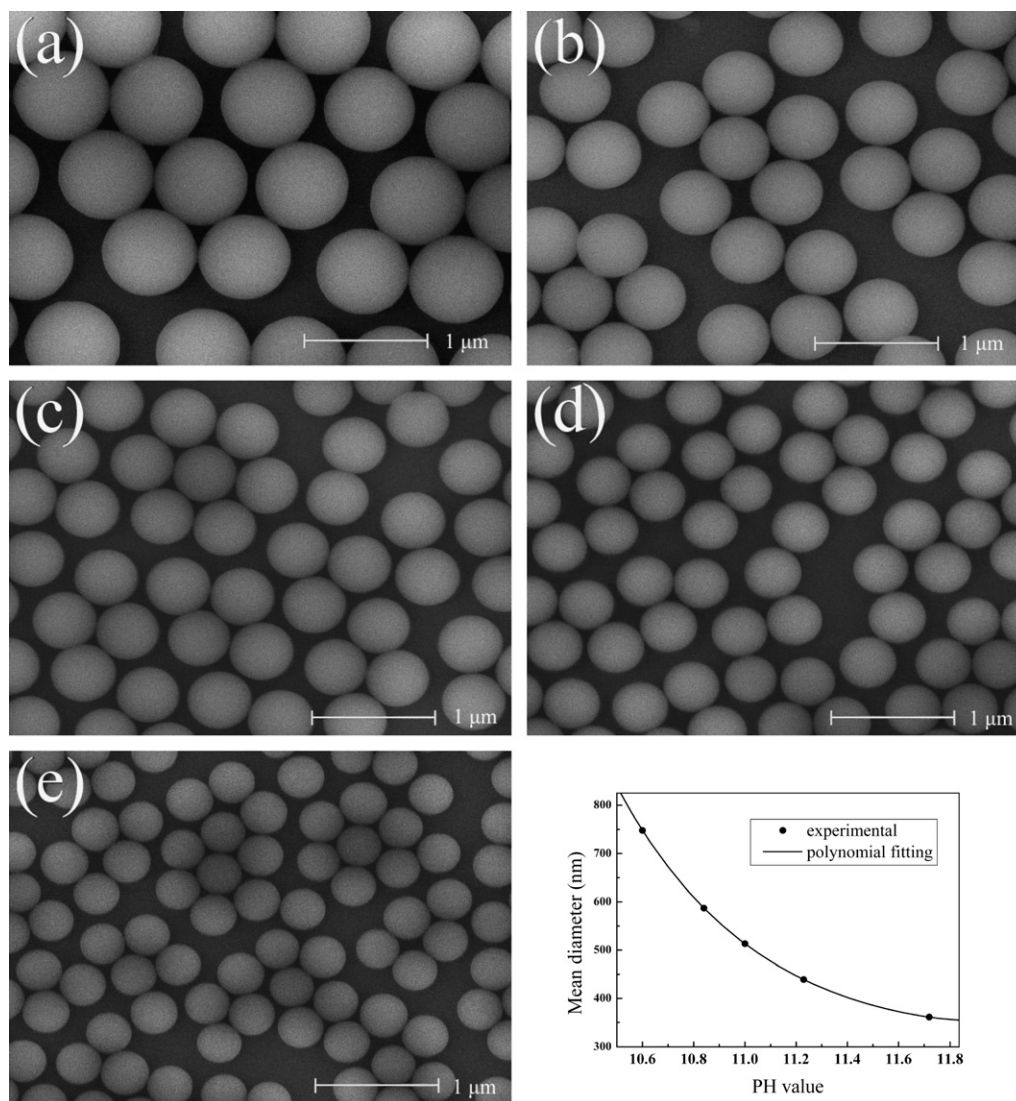


**Fig. 6.** SEM images of monodisperse hybrid silica spheres prepared using 3 mL VTES in 50 mL H<sub>2</sub>O by adding various amounts of ammonia: (a) 0.025 mL, (b) 0.1 mL, (c) 0.2 mL, (d) 0.5 mL and (e) 5 mL, respectively. The resultant particle sizes are (a) 748 nm, (b) 587 nm, (c) 513 nm, (d) 439 nm, and (e) 361 nm. The plot shows the inverse relationship between the particle size and the pH value, that is, the particle size decreases with the increase of pH value. The reaction was carried out under constant stirring rate at room temperature ( $22 \pm 1^\circ\text{C}$ ).

the particle size. By adding the ammonia solution from 0.025 to 5 mL (the pH value varied from 10.60 to 11.72), the particle size changes from  $\sim 750$  to  $\sim 360$  nm. The plot in Fig. 6 shows the inverse relationship between the particle size and the pH value, that is, the particle size decreases with the increase of pH value. When the pH value was 10.60, highly monodisperse hybrid silica spheres were obtained with the size of 748 nm. A little increase in pH value to 10.84 resulted in soon decreasing the particle size to 587 nm. With a further increase in pH values to 11, 11.23 and 11.72, the resultant particle sizes were obtained to 513, 439 and 361 nm, respectively. With the increase of pH value, the decreasing trend of particle size became slowly. It was found that the pH value had to be higher than 10.60 in order to make the reaction proceed successfully. The obvious agglomeration would occur at pH values below 10.60, and no sub-micrometer spheres could be obtained. The detailed explanation about the inverse relationship between the particle size and the pH value will be given in the next part.

### 3.3. The formation mechanism of colloidal spheres

Based on the classical nucleation theory [30], if nucleation induced spontaneously without any seed (dust particles or bubbles),

the homogeneous nucleation could be realized. The free energy changes associated with the process of homogeneous nucleation may be considered as follows: The Gibbs free energy of formation of spherical crystals with radius  $r$  from the solution with supersaturation  $S$  is given in equation:

$$\Delta G = 4\pi r^2 \gamma + \frac{4}{3}\pi r^3 \Delta G_v, \quad (1)$$

$\gamma$  is the interfacial tension, which represents the surface free energy per unit area, is always positive.  $\Delta G_v$  is the excess free energy between a very large particle ( $r \rightarrow \infty$ ) and the solute in solution. Because

$$\Delta G_v = \frac{(-RT \ln S)}{V}$$

where  $V$  is the molecular volume of the bulk crystal;  $\Delta G_v$  is negative as long as the solution is supersaturated ( $S > 1$ ). So the  $\Delta G$  has a maximum, setting

$$\frac{d\Delta G}{dr} = 0.$$

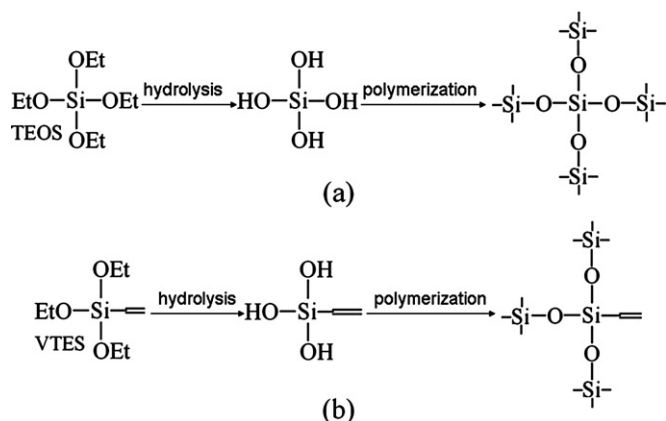


**Fig. 7.** Schematic illustration of the formation of (a) pure silica spheres and (b) hybrid silica spheres. They both experience the hydrolysis and polycondensation period.

Thus we can get the critical radius:

$$r_c = \frac{-2\gamma}{\Delta G_v} = \frac{-2\gamma V}{RT \ln S}. \quad (2)$$

This is the minimum radius of a nucleus that can grow spontaneously in the supersaturated solution. Because  $r_c$  is the minimum radius that will persist and not dissolve away in solution,  $S$  should be sufficiently high for  $r_c$  to be smaller than the size of the crystal embryos that form the nuclei for the homogeneous nucleation process [31].

LaMer and Dinegar [32] prepared a colloidal dispersion by condensation from initially supersaturated solution and developed a theory which accounted for the production of monodisperse colloids. According to their literature, in a sufficient supersaturated solution, many nuclei are generated simultaneously, and then these nuclei start to grow without additional nucleation. The experiences of particles growth are nearly the same because all of the particles nucleate almost simultaneously. This process makes it possible to control the size distribution of the ensemble of particles as a whole during growth.

The schematic illustration of the formation of monodisperse pure silica spheres and hybrid silica spheres are given in Fig. 7. Each reaction scheme is a simplification of the complex condensation processes that lead to the formation of the pure silica spheres or hybrid silica spheres. In the synthesis of pure silica, two main types of reactions are involved: (1) silanol groups are formed by hydrolysis and (2) siloxane bridges are formed by a polycondensation reaction [33]. Similarly, we can give a compendious explanation in the formation mechanism of the monodisperse hybrid silica spheres synthesized by VTES precursor. A VTES molecule has three ethoxyl groups. They are easily changed to hydroxyl groups on proper condition. Although the VTES/water solution was turbid at the beginning of the stage, it appeared transparently after  $\sim 2$  h vigorous magnetic stirring. The VTES hydrolyzed in the process and released ethanol which could help the VTES to be completely dissolved in water medium [10,14]. In the presence of ammonia the supersaturation  $S$  achieved sufficiently high. Then the polycondensation was generated and monodisperse spherical colloids of hybrid silica with vinyl group could be obtained. However, the TEOS cannot realize the dissolved process in pure water solution (we attempted it and failed). Therefore, ethanol must be used for dissolving the TEOS.

Let us now look in detail into the influence of the reaction conditions on the particle size. Being the source of monomer, concentration of VTES will determine the concentration of nuclei particles present in the system. At initial period, nucleation will take place and will induce the formation of primary particles in the pres-

ence of ammonia. Polycondensation of primary particles results in the formation of more stable larger particles. The process will continue until all the nuclei consumed or until a stable condition is achieved. Under the constant concentration of ammonia, increase of the amount of VTES will lead to extending the growth period. The longer growth takes place resulting in the larger particle size. In many previous studies, the same result was observed [34–36]. When the VTES concentration was too low, the solution could not reach sufficient supersaturation. Consequently, homogeneous nucleation could not be realized on this condition, and only crumpled particles could be formed.

According to Matsoukas and Gulari [37–39], the larger particles were obtained by increasing the concentration of ammonia. The effect of ammonia concentration is to promote hydrolysis, but also to promote the polycondensation rate, resulting in faster kinetics, and larger particle sizes.

However, a reverse effect that the small particle size was obtained in the higher ammonia concentration (pH value), was observed in our experiments. We can explain this as follow. When the ammonia is added in the VTES/water solution, the nuclei are generated immediately. Soon after the homogeneous nucleation process, the growth process of colloidal crystal of hybrid silica proceeds. With the increase of pH value, the nucleation rate becomes faster so that the more nuclei are generated. Consequently, the particle size relatively decreases due to high nucleation rate. Although the polycondensation rate also becomes faster, it has few effect compared with the nucleation rate. When the pH value is relatively lower, increase of the nucleation rate is obvious with the increase of the ammonia concentration. As a result, quantities of the nuclei increase largely and the particle size decreases rapidly. At a relatively higher pH value, increase of the nucleation rate is unobvious so that the resultant particle size decreases slowly. The analysis of the homogeneous nucleation and growth processes greatly interprets the inverse relationship between the particle size and the pH value (see plot in Fig. 6).

### 3.4. The method of measuring polydispersity ( $\sigma_r$ )

To measure reliably such low polydispersity is challenging. Commonly photon correlation spectroscopy (PCS is also known as dynamic light scattering (DLS) or quasi-elastic light scattering (QELS)) method is used to measure particle size and distribution. In detecting the distribution, the experimental plot has to be analyzed as all dispersions have some degree of polydispersity. The problem is that we cannot obtain a unique solution when we try and invert the summation [40]. Although the instrument manufacturers try to calibrate against particles of known size, the problem cannot be totally solved. Thus the reliability of distribution cannot be ensured. As pointing toward a strong particle swelling or chain expansion at the particle surfaces, it always gives a larger particle size than does the SEM method [13,14,41]. Additionally, it has a limitation that the particles must be dispersed in the solution.

However, SEM is the direct method of measuring polydispersity since PCS can hardly be used for sedimenting large silica spheres [28]. The SEM (Tecnai XL30 SFEG) has a stable imaging state after calibration by the manufacturer, so under the same magnification the deviation among the images can be neglected. Moreover, particles in one image have one magnification, and the deviation can also be neglected among particles in one image. The relative error (e.g., for measuring the same sphere twice) should not exceed 1.5%. Upon several repeated measurements, the realistic error estimate is 1%. Thus the reliability of distribution can be ensured. We measured about two hundred spheres for each sample to collect a statistically meaningful sample size. The resultant  $\sigma_r$  is at least 1.9% or better as listed in Table 1.



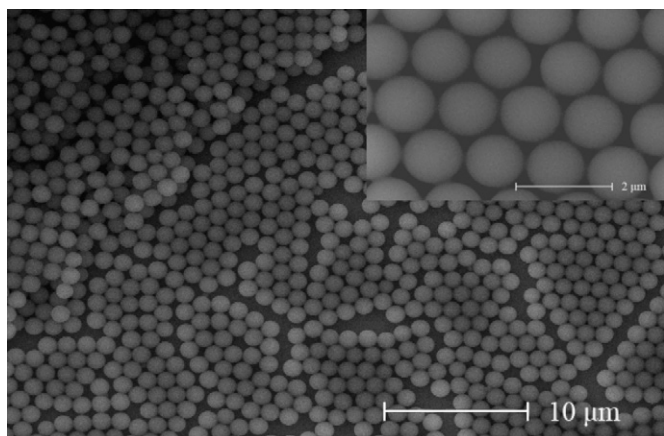


**Fig. 8.** SEM image of MPTMS hybrid silica spheres (1282 nm in mean diameter) fabricated by 3 mL MPTMS and 50 mL H<sub>2</sub>O by adding 0.2 mL ammonia solution. The inset shows a closer look on the surface of hybrid silica spheres. The reaction was carried out under constant stirring rate at room temperature ( $22 \pm 1^\circ\text{C}$ ).

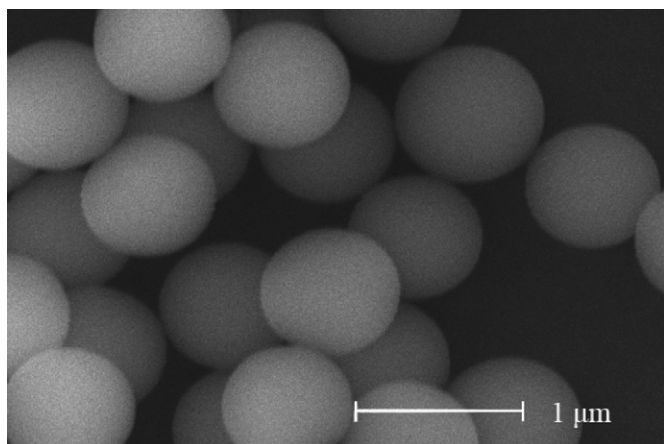


**Fig. 9.** SEM image of PTES hybrid silica spheres (830 nm in mean diameter) fabricated by 3 mL PTES and 50 mL H<sub>2</sub>O by adding 0.2 mL ammonia solution. The reaction was carried out under constant stirring rate at room temperature ( $22 \pm 1^\circ\text{C}$ ).

### 3.5. MPTMS and PTES hybrid silica spheres

This method has also been extended to design and prepare other hybrid silica spheres. Lee et al. [20] prepared monodisperse hybrid MPTMS silica spheres using a one-step sol–gel reaction in aqueous solution. The results of the MPTMS and PTES silica spheres were shown in Figs. 8 and 9. Fig. 8 shows the SEM image of MPTMS hybrid silica spheres prepared using sol–gel process. The particle size was 1282 nm (with  $\sigma_r = 1.33\%$ ). Compared with the VTES silica spheres, the MPTMS silica spheres also indicated the abundance in quantity, the uniformity in size/shape, and the smoothness on surfaces (see the inset in Fig. 8). Fig. 9 shows the SEM image of PTES hybrid silica spheres with 830 nm in mean diameter. The monodispersity of PTES silica spheres ( $\sigma_r = 3.80\%$ ) is not as good as the monodispersity of VTES/MPTMS silica spheres. The reason is that the synthetic condition of MPTMS was the same as the VTES's. But in the case of preparing PTES silica spheres, a few amount of Tween 20 was added. The precursor PTES has a hydrophobic phenyl, it is difficult to dissolve in water solution. To disperse PTES in water solution, a surfactant (Tween 20) was used. Because the mixture was emulsion phase after adding Tween 20, the PTES were not completely dissolved in the emulsion. As a result, the PTES silica spheres with low monodispersity were obtained.

## 4. Summary

We have demonstrated an effective and reproducible method for preparing highly monodisperse organic–inorganic hybrid silica spheres synthesized by an organosilane with controllable size in aqueous solution using only one process. FT-IR and  $^{29}\text{Si}$  NMR spectra confirm the existence of vinyl group ( $-\text{CH}=\text{CH}_2$ ) and that the vinyl group connects to the silicon atom. This method is remarkable for its simplicity (*one process, one precursor and one solvent*); for its good control of the size, uniformity and stability of hybrid silica spheres; and for its self-hydrolysis ability to realize homogeneous nucleation of silica, fast reaction and reproducibility. The size of hybrid silica spheres could be adjusted from 360 to 770 nm with  $\sigma_r$  below 2% by controlling the concentration of VTES precursor and ammonia catalyst. To get the smooth and spherical hybrid silica particles, the volume ratio of the VTES and water should be above 1:50, while the pH value has to be higher than 10.60 in order to make the reaction proceed successfully. The increasing of the precursor concentration increases the particle size while the pH value has a reverse effect on the particle size. The homogeneous nucleation and growth processes have been discussed, and a compendious explanation have been given in the formation mechanism of the highly monodisperse hybrid silica spheres. The knowledge gained from this study will be useful and convenient in the design and preparation of organic–inorganic hybrid materials especially in monodisperse surface-modified silica spheres. The highly monodisperse hybrid silica spheres are expected to find more uses as biocatalyst, surface modification, and assembly of photonic crystals.

## Acknowledgment

This work is supported by the NSFC 50672002.

## References

- [1] A.P. Wight, M.E. Davis, Chem. Rev. 102 (2002) 3589.
- [2] J. Park, J. Joo, S.G. Kwon, Y. Jang, T. Hyeon, Angew. Chem. Int. Ed. 46 (2007) 4630.
- [3] A.S.M. Chong, X.S. Zhao, A.T. Kustedjo, S.Z. Qiao, Microporous Mesoporous Mater. 72 (2004) 33.
- [4] A.S.M. Chong, X.S. Zhao, Catal. Today 93–95 (2004) 293.
- [5] A.S.M. Chong, X.S. Zhao, Appl. Surf. Sci. 237 (2004) 398.
- [6] F.W. Fabris, F.C. Stedile, R.S. Mauler, S.M.B. Nachtigall, Eur. Polym. J. 40 (2004) 1119.
- [7] V. Uricanu, D. Donescu, A.G. Banu, S. Serban, M. Olteanu, M. Dudau, Mater. Chem. Phys. 85 (2004) 120.
- [8] E.J. Nassar, E.C.O. Nassor, L.R. Ávila, P.F.S. Pereira, A. Cestari, L.M. Luz, K.J. Ciuffi, P.S. Calefi, J. Sol–Gel Sci. Technol. 43 (2007) 21.
- [9] P. Toro, R. Quijada, O. Murillo, M. Yazdani-Pedram, Polym. Int. 54 (2005) 730.
- [10] S. Jain, J.G.P. Goossens, M. Duin, Macromol. Symp. 233 (2006) 225.
- [11] C.C. M. Ma, Y.J. Chen, H.C.J. Kuan, Appl. Polym. Sci. 98 (2005) 2266.
- [12] X.L. Xie, C.Y. Tang, X.P. Zhou, Y. Li, Z.Z. Yu, Q.X. Zhang, Y.W. Mai, Chem. Mater. 16 (2004) 133.
- [13] M. Khiterer, K.J. Shea, Nano Lett. 7 (2007) 2684.
- [14] Z.J. Wu, H. Han, W. Han, B. Kim, K.H. Ahn, K. Lee, Langmuir 23 (2007) 7799.
- [15] Z.J. Wu, H. Xiang, T. Kim, M.S. Chun, K. Lee, J. Colloid Interface Sci. 304 (2006) 119.
- [16] W. Wang, B. Gu, L. Liang, W.A. Hamilton, J. Phys. Chem. B 107 (2003) 12113.
- [17] W. Wang, B. Gu, L. Liang, W.A. Hamilton, J. Phys. Chem. B 107 (2003) 3400.
- [18] W. Wang, B. Gu, J. Phys. Chem. B 109 (2005) 22175.
- [19] W. Wang, B. Gu, L. Liang, J. Colloid Interface Sci. 313 (2007) 169.
- [20] Y.G. Lee, J.H. Park, C. Oh, S.G. Oh, Y.C. Kim, Langmuir 22 (2007) 10875.
- [21] W. Stöber, A. Fink, E. Bohn, J. Colloid Interface Sci. 26 (1968) 62.
- [22] L. King, A.C. Sullivan, Chem. Rev. 189 (1999) 19.
- [23] M.P. Vinod, D. Bahenemann, P.R. Rajamohanam, K. Vijayamohanam, J. Phys. Chem. B 107 (2003) 11583.
- [24] D.W. Sindorf, G.E. Maciel, J. Am. Chem. Soc. 103 (1981) 4263.
- [25] D.W. Sindorf, G.E. Maciel, J. Am. Chem. Soc. 105 (1983) 3767.
- [26] I. Chuang, D.R. Kinney, G.E. Maciel, J. Am. Chem. Soc. 115 (1993) 8695.
- [27] R. Joseph, S. Zhang, W.T. Ford, Macromolecules 29 (1996) 1305.
- [28] S. Wong, V. Kitaev, G.A. Ozin, J. Am. Chem. Soc. 125 (2003) 15589.

- [29] D. Nagao, H. Osuzu, A. Yamada, E. Mine, Y. Kobayashi, M. Konno, J. Colloid Interface Sci. 279 (2004) 143.
- [30] J.W. Mullin, *Crystallization*, third ed., Oxford Univ. Press, Oxford, 1997.
- [31] L. Spanhel, M.A. Anderson, J. Am. Chem. Soc. 113 (1991) 2826.
- [32] V.K. LaMer, R.H. Dinegar, J. Am. Chem. Soc. 72 (1950) 4847.
- [33] K.S. Rao, K.E. Hami, T. Kodaki, K. Matsushige, K. Makino, J. Colloid Interface Sci. 289 (2005) 125.
- [34] G.H. Bogush, M.A. Tracy, C.F. Zukoski, J. Non-Cryst. Solids 104 (1988) 95.
- [35] G.H. Bogush, C.F. Zukoski, J. Colloid Interface Sci. 142 (1991) 1.
- [36] G.H. Bogush, C.F. Zukoski, J. Colloid Interface Sci. 142 (1991) 19.
- [37] T. Matsoukas, E. Gulari, J. Colloid Interface Sci. 124 (1988) 252.
- [38] T. Matsoukas, E. Gulari, J. Colloid Interface Sci. 132 (1989) 13.
- [39] T. Matsoukas, E. Gulari, J. Colloid Interface Sci. 145 (1991) 557.
- [40] J.W. Goodwin, *Colloids and Interfaces with Surfactants and Polymers: An Introduction*, Wiley, West Sussex, 2004.
- [41] C.A.R. Costa, C.A.P. Leite, F. Galembeck, J. Phys. Chem. B 107 (2003) 4747.